High-Efficiency DC-DC Converter With High Voltage Gain and Reduced Switch Stress

Rong-Jong Wai, *Senior Member, IEEE*, Chung-You Lin, Rou-Yong Duan, and Yung-Ruei Chang, *Member, IEEE*

***Abstract*—In this paper, a high-efficiency dc-dc converter with high voltage gain and reduced switch stress is proposed. Generally speaking, the utilization of a coupled inductor is useful for raising the step-up ratio of the conventional boost converter. However, the switch surge voltage may be caused by the leakage inductor so that it will result in the requirement of high-voltage-rated devices. In the proposed topology, a three-winding coupled inductor is used for providing a high voltage gain without extreme switch duty-cycle and enhancing the utility rate of magnetic core. Moreover, the energy in the leakage inductor is released directly to the output terminal for avoiding the phenomenon of circulating current and the production of switch surge voltage. In addition, the delay time formed with the cross of primary and secondary currents of the coupled inductor is manipulated to alleviate the reverse-recovery current of the output diode. It can achieve the aim of high-efficiency power conversion. Furthermore, the closed-loop control methodology is utilized in the proposed scheme to overcome the voltage drift problem of the power source under the variation of loads. Some experimental results via an example of a proton exchange membrane fuel cell power source with 250-W nominal rating are given to demonstrate the effectiveness of the proposed power conversion strategy.**

***Index Terms*—DC-DC converter, coupled inductor, fuel cell, proton exchange membrane, reverse recovery.**

I. Introduction

In RECENT, dc-dc converters with steep voltage ratio are usually required in many industrial applications. For examples, the front-end stage for clean-energy sources, the dc back-up energy system for an uninterruptible power supply (UPS), high-intensity discharge lamps for automobile headlamps, and telecommunication industry [1]–[3]. The conventional boost converters cannot provide such a high dc voltage ratio due to the losses associated with the inductor, filter capacitor, switch and output diode. Even for an extreme duty cycle, it will result in serious reverse-recovery problems and increase the rating of the output diode. As a result, the conversion efficiency is degraded and the electromagnetic interference (EMI) problem is severe under this situation [4]. In order to increase the conversion efficiency and voltage gain, many modified boost converter topologies have been investigated in the past decade [5]–[13].

Although voltage-clamped techniques are manipulated in the converter design to overcome the severe reverse-recovery problem of the output diode in high-level voltage applications, there still exists overlarge switch voltage stresses and the voltage gain is limited by the turn-on time of the auxiliary switch [5], [6]. Silva *et al.* [7] presented a boost soft-single-switch converter, which has only one single active switch. It is able to operate with soft switching in a pulse-width-modulation (PWM) way without high voltage and current stresses. Unfortunately, the voltage gain is limited below four in order to achieve the function of soft switching. In [8] and [9], coupled inductors were employed to provide a high step-up ratio and to reduce the switch voltage stress substantially, and the reverse-recovery problem of the output diode was also alleviated efficiently. In this case, the leakage energy of the coupled inductor is another problem as the switch was turned off. It will result in the high-voltage ripple across the switch due to the resonant phenomenon induced by the leakage current. In order to protect the switch devices, either a high-voltage-rated device with higher $R_{\mathrm{DS(on)}}$ or a snubber circuit is usually adopted to deplete the leakage energy. By these ways, the power conversion efficiency will be degraded. Zhao and Lee [10] introduced a family of high-efficient and high step-up dc-dc converters by only adding one addition diode and a small capacitor. It can recycle the leakage energy and alleviate the reverse-recovery problem. In this scheme, the magnetic core can be regarded as a flyback transformer and most of the energy was stored in the magnetic inductor. However, the capacity of the magnetic core should be increased substantially when the demand of high output power is required. Ivanovic and Stojikovic [11] presented a novel active snubber for the boost converter, where the auxiliary switch was taken part in energy transfer from source to output. However, two switches were required to provide a high step-up ratio. Wai and Duan [12] introduced a high-efficiency converter with high voltage gain, which has only one active switch. Unfortunately, the phenomenon of circulating current is a latent problem to be solved. Wai *et al.* [13] investigated a high-efficiency voltage-clamped dc-dc converter with reduced reverse-recovery current and switch-voltage stress. In this circuit topology, it was designed by way of the combination of inductor and transformer to increase the corresponding voltage gain. The requirement of an additional inductor and a coupled inductor with higher coupling coefficient will increase the manufacturing difficulty and productive cost.

Nowaday, fuel cells are in the news because they appear to be one of the most efficient and effective solutions to the environmental pollution problem [14]–[20]. A fuel cell is an

Manuscript received October 17, 2004; revised May 16, 2006. Abstract published on the Internet November 30, 2006. This work was supported in part by the Institute of Nuclear Energy Research of Taiwan, R.O.C. under Grant NL950206 and in part by the Ministry of Education of Taiwan, R.O.C. under Grant MOE 0950026846.

R.-J. Wai and C.-Y. Lin are with the Department of Electrical Engineering, Yuan Ze University, Taiwan 32026, R.O.C. (e-mail: rjwai@saturn.yzu.edu.tw).

R.-Y. Duan is with the Department of Industrial Safety & Health, Hung Kuang University, Taiwan 43302, R.O.C.

Y.-R. Chang is with the Institute of Nuclear Energy Research, Atomic Energy Council, Taiwan 32546, R.O.C.

Digital Object Identifier 10.1109/TIE.2006.888794

energy conversion device that produces electricity by electrochemically combining fuel (hydrogen) and oxidant (oxygen from the air) gases through electrodes, across an ion conductive electrolyte. This process produces much higher conversion efficiency than any conventional thermal-mechanical system because the system operates without combustion and extracts more electricity from the same amount of fuel. This system has the merits of high efficiency, energy security (i.e., reduce oil consumption, cut oil imports, and increase the amount of the country's available electricity supply), reliability, pollution free and quiet operations [17]. Fuel cells have been known to science for more than 160 years and have recently become the subject of intense research and development. Up to now, many demonstration projects have shown fuel cell systems to be feasible for portable power, transportation, utility power and on-site power generation in a variety of building applications.

As portable power supply, a fuel cell with a fuel container can offer a higher energy density and more convenience than conventional battery systems. Moreover, portable power packs using fuel cells can be lighter and smaller in volume for an equivalent amount of energy. In transportation applications, fuel cells offer higher efficiency and better load performance than conventional engines. In stationary power applications, low emissions permit fuel cells to be located in high-power requirement areas where they can supplement the existing utility grid. Using fuel cells and hydrogen technology, electrical power can be delivered wherever and whenever required, cleanly, efficiently, and with sustainability if the fuel is sufficient. The greatest research interests throughout the world have focused on proton exchange membrane (PEM) and solid oxide fuel cell (SOFC) stacks. In special, the PEMFC has promising characteristics as follows: 1) the by-product waste is water; 2) low-temperature operation; 3) they use a solid polymer as the electrolyte that reduces concerns related to construction, transportation, and safety issues [19]. According to documentary reports [17], fuel cells can convert up to 50%–70% of available fuel to electricity (90% with heat recovery). PEMFC is a well-advanced type of fuel cell suitable for cars and mass transportation if it can be made cost competitive and the problems of electrodes poison and water management can be appropriately solved. Its efficiency is around 50% which is better than internal combustion engines.

The aim of this study is to design a high-efficiency dc-dc converter with high voltage gain and reduced switch stress to provide a stable constant dc voltage. To achieve this goal, the manipulation of a three-winding coupled inductor is adopted to increase the voltage gain and to enhance the utility rate of magnetic core. Moreover, the problem of the leakage inductor and the reverse recovery in the conventional boost converter also can be solved so that it can achieve the aim of high-efficiency power conversion. In addition, the feedback control methodology is utilized in the proposed converter to overcome the voltage drift problem of the power source under the variation of loads. The prototype is developed for a PEMFC application requiring an output power of 300 W, an output voltage 400 V and an input voltage varying from 27 V to 36.5 V. The remainder of this study is organized as follows. Section II presents the converter design and analyses in detail. In Section III, the PEMFC operation principle is introduced briefly. Experimental results for a PEMFC power source with 250-W nominal rating are provided to validate the effectiveness of the proposed power conversion system in Section IV. Conclusions are drawn in Section V.

II. Converter Design and Analyses

The system configuration of the proposed converter topology is depicted in Fig. 1(a), where it contains six parts including a dc input circuit, a primary-side circuit, a secondary-side circuit, a third-side circuit, a dc output circuit and a feedback control mechanism. The major symbol representations are summarized as follows. V_i and I_i denote the dc input voltage and current, and C_i is the input capacitor in the dc input circuit. L_1, L_2, and L_3 represent the individual inductors in the primary-side, secondary-side, and third-side of the three-winding coupled inductor, respectively. S is the switch in the primary-side circuit. C_2 and D_2 are the clamped capacitor and rectifier diode in the secondary-side circuit. C_3 and D_3 are the clamped capacitor and rectifier diode in the third-side circuit. V_0 and I_0 describe the output voltage and current; R_0 is the output load; D_0 and C_0 are the output diode and filter capacitor in the output circuit. v_g is the trigger signal in the feedback control mechanism.

The equivalent circuit and state definition of the newly designed converter is depicted in Fig. 1(b), where the three-winding coupled inductor is modeled as a 1-to-2 ideal transformer with a magnetizing inductor (L_m) and an equivalent leakage inductor (L_k). The turn ratios of this ideal transformer are defined as

$$n_2 = \frac{N_2}{N_1} \tag{1}$$

$$n_3 = \frac{N_3}{N_1} \tag{2}$$

where N_1, N_2, and N_3 are the primary-side, secondary-side, and third-side winding turns, respectively. For simplicity, the dc input circuit in Fig. 1(a) is denoted as a constant voltage source, V_s. The voltages across the switch, the primary winding of the ideal transformer, and the equivalent leakage inductor are v_{ds}, v_{N1} and v_{Lk}, respectively. The clamped capacitors, C_2 and C_3, are assumed to be large enough to view as constant voltage sources, V_{c2} and V_{c3}. Moreover, the conductive voltage drops of the switch (S) and all diodes (D_0, D_2, and D_3) are neglected to simplify circuit analyses. The characteristic waveforms of the proposed high-efficiency converter are depicted in Fig. 2. In addition, Fig. 3 illustrates the topological modes in one switching cycle and the detailed operation stages are described as follows.

A. Mode 1 $(t_0 - t_1)$ [Fig. 3(a)]

At time $t = t_0$, the switch (S) is turned on. At the same time, the diode (D_3) becomes conducting, and the diodes (D_0 and D_2) are reverse-biased. The clamped capacitor (C_3) is linearly charged by the input voltage source (V_i) through the coupled inductor. Applying Kirchhoff's law [4], the change rate of the third-side current (i_{D3}), the magnetizing inductor current (i_{Lm})

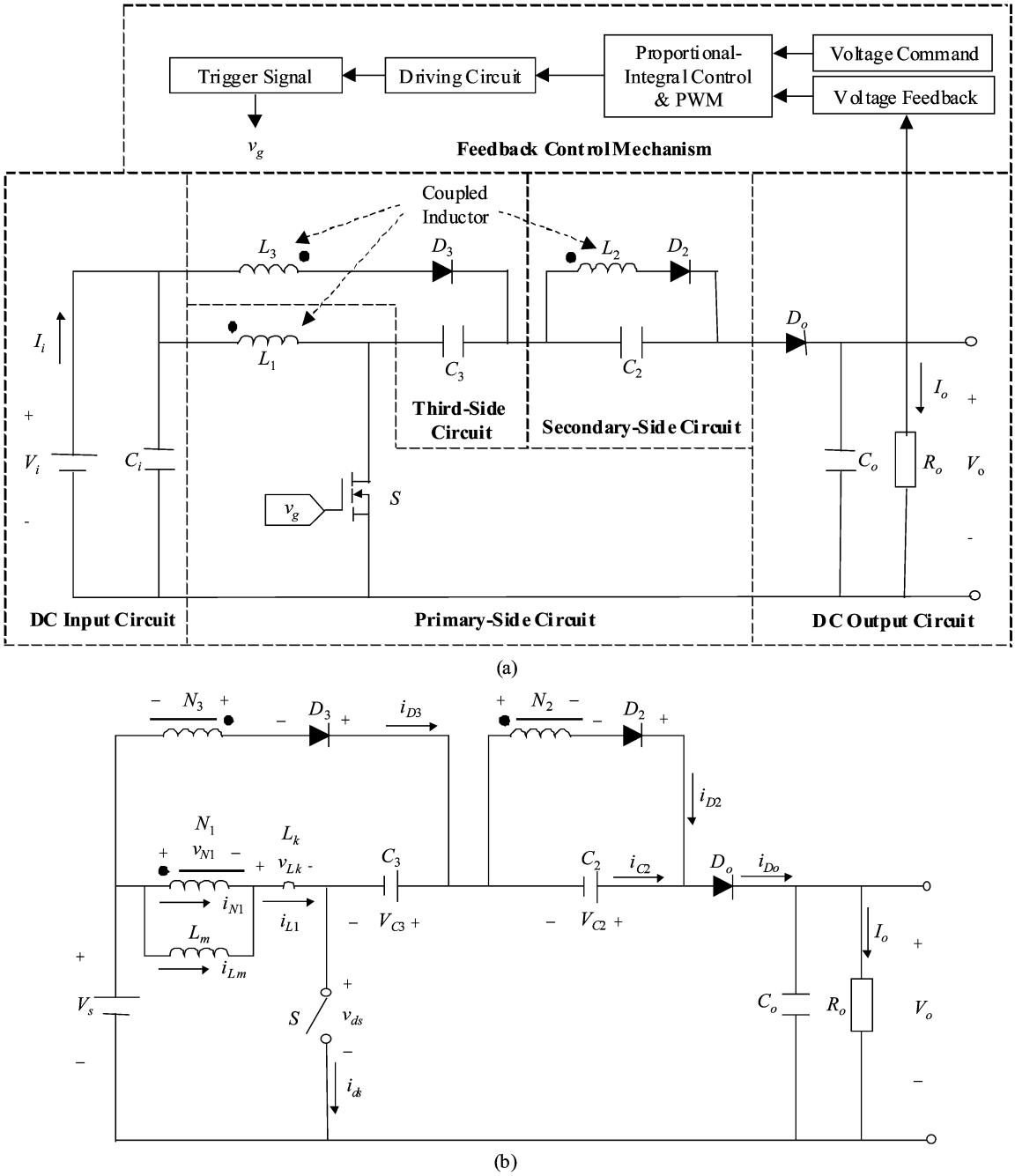

Fig. 1. High-efficiency dc-dc converter: (a) System configuration; (b) Equivalent circuit scheme.

and the primary-side current (i_{L1}) of the coupled inductor can be represented as

$$\frac{di_{D3}}{dt} = \frac{n_3 V_s - (V_{C3} - V_s)\left(1 + \frac{L_k}{L_m}\right)}{n_3^2 L_k} \tag{3}$$

$$\frac{di_{Lm}}{dt} = \frac{V_{C3} - V_s}{n_3 L_m} \tag{4}$$

$$\frac{di_{L1}}{dt} = \frac{(1+n_3)V_s - V_{C3}}{n_3 L_k}. \tag{5}$$

Moreover, the voltage across the magnetizing inductor (v_{Lm}) can be denoted as

$$v_{Lm}(t) = v_{N1}(t) = \frac{V_{C3} - V_s}{n_3}. \tag{6}$$

In Mode 1, the energy from the input power source is stored in the magnetizing inductor (L_m), equivalent leakage inductor (L_k), and clamped capacitor (C_3)

B. Mode 2 $(t_1 - t_2)$ [Fig. 3(b)]

At time $t = t_1$, the switch (S) is turned off. At this time, the diodes (D_0 and D_2) become forward-biased to start con-

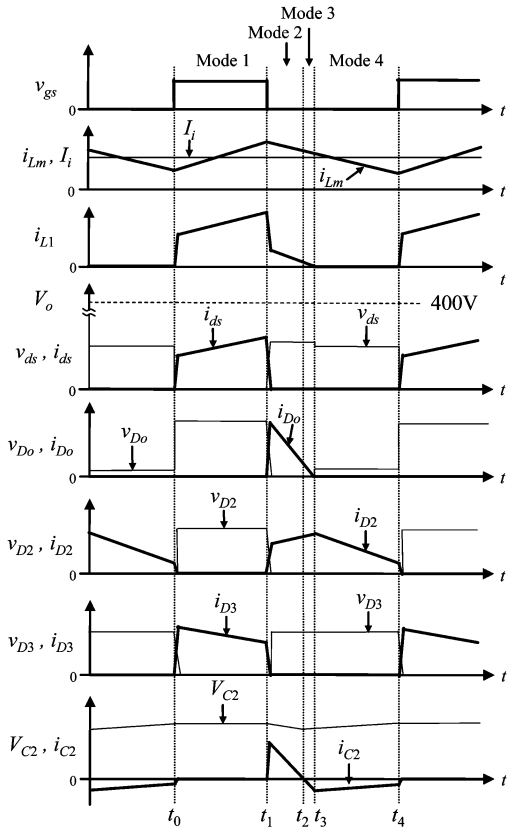

Fig. 2. Characteristic waveforms of high-efficiency dc-dc converter.

ducting and the diode (D_3) is reverse-biased. The stored energy of the magnetizing inductor (L_m) and equivalent leakage inductor (L_k) in Mode 1 is released to output loads through the clamped capacitors (C_2 and C_3). Moreover, the ideal transformer through the secondary-side transits the energy in the magnetizing inductor (L_m) to the output terminal by way of magnetic coupling. Applying Kirchhoff's law [4], the voltage relations during this mode can be described by

$$v_{ds}(t) + V_{C2} + V_{C3} = V_o \tag{7}$$

$$V_{C2} = -n_2 \cdot v_{N1}(t) \tag{8}$$

$$v_{Lm}(t) = v_{N1}(t) = -\left[\frac{V_o + v_{Lk}(t) - V_s - V_{C3}}{1+n_2}\right]. \tag{9}$$

Simultaneously, the switch voltage stress can be calculated as

$$v_{ds}(t) = V_s - v_{N1}(t) - v_{Lk}(t) = V_o - V_{C2} - V_{C3} < V_o. \tag{10}$$

According to (10), the cutoff voltage of the switch (S) is clamped at $V_o - V_{C2} - V_{C3}$. Moreover, the switch (S) with low-voltage-rated capacity can be selected since the switch voltage stress (v_{ds}) is smaller than the output voltage (V_0). The selection of a low-voltage-rated device with lower $R_{\mathrm{DS(on)}}$ is useful for improving the conversion efficiency. Refer to (7)–(9), the currents (i_{Lm}, i_{L1}, i_{D2}, and i_{C2}) are at the rate of

$$\frac{di_{Lm}}{dt} = -\left(\frac{v_{C2}}{n_2 L_m}\right) \tag{11}$$

$$\frac{di_{L1}}{dt} = \frac{n_2(-V_o + V_s + V_{C3}) + (1+n_2)V_{C2}}{n_2 L_k} \tag{12}$$

$$\frac{di_{D2}}{dt} = \frac{n_2(V_o - V_s - V_{C3}) - \left(1 + n_2 + \frac{L_k}{L_m}\right)V_{C2}}{n_2^2 L_k} \tag{13}$$

$$\frac{di_{C2}}{dt} = (1+n_2)\frac{n_2(-V_o + V_s + V_{C3}) + (1+n_2)V_{C2}}{n_2^2 L_k} + \frac{V_{C2}}{n_2^2 L_m} \tag{14}$$

where i_{D2} is the secondary-side current of the coupled inductor, and i_{C2} is the current passed through the clamped capacitor (C_2) in the secondary-side circuit.

C. Mode 3 $(t2 - t3)$ [Fig. 3(c)]

At time $t = t_3$, the residual energy of the clamped capacitor (C_2) is discharged entirely, i.e., $i_{C2}(t_2)$. Immediately, the clamped capacitor (C_2) is charged by the energy of the magnetizing inductor (L_m) through the ideal transformer. Thus, the value of i_{C2} is negative and its change rate is the same as (14). Moreover, the stored energy in the clamped capacitor (C_3) is released continuously to the output terminal and its change rate is the same as (12). Note that, the currents in the series path decay gradually with respect to time.

D. Mode 4 $(t3 - t4)$ [Fig. 3(d)]

At time $t = t_3$, the primary-side current of the coupled inductor decays to zero (i.e., $i_{L1}(t_3) = 0$), and the energy stored in the coupled inductor is represented by the secondary-side current. At this time, the output diode (D_0) is reverse-biased and the output diode current (i_{D0}) decays to zero. It can alleviate the reverse-recovery problem within the output diode (D_0). In the meantime, the clamped capacitor (C_2) is charged continuously by the energy of the magnetizing inductor (L_m) through the ideal transformer. The magnetizing inductor current (i_{Lm}) is decayed linearly and its change rate is similar to (11). Moreover, the rate of change of the charge current passes through the clamped capacitor (C_2) can be represented as

$$\frac{di_{C2}}{dt} = -\frac{di_{D2}}{dt} = \frac{V_{C2}}{n_2^2 L_m} \tag{15}$$

The current of i_{D2} is proportional to the magnetizing inductor current (i_{Lm}). During this period, the leakage inductor current (i_{L1}) is zero until the switch (S) is turned on. Since the leakage inductor voltage (v_{Lk}) is equal to zero, the switch voltage (v_{ds}) can be described as

$$v_{ds}(t) = V_s - v_{N1}(t). \tag{16}$$

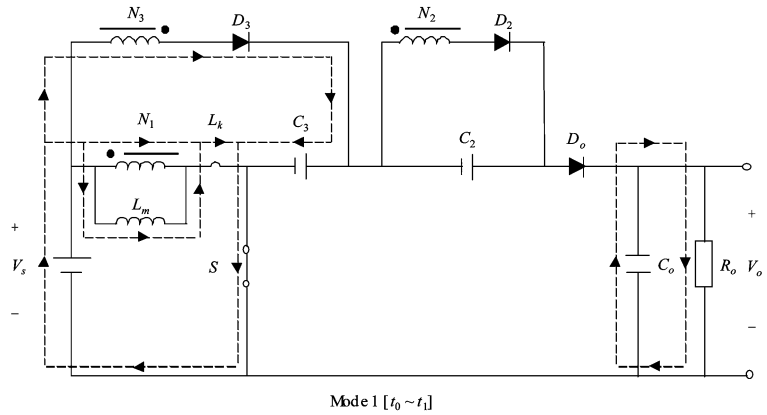

Mode 1 $[t_0 \sim t_1]$

(a)

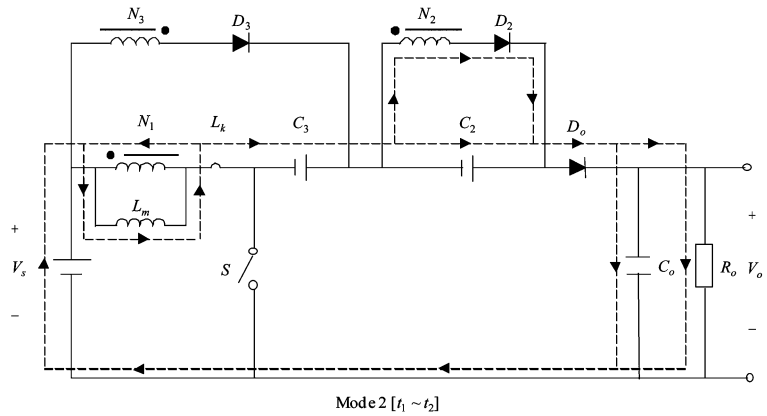

Mode 2 $[t_1 \sim t_2]$

(b)

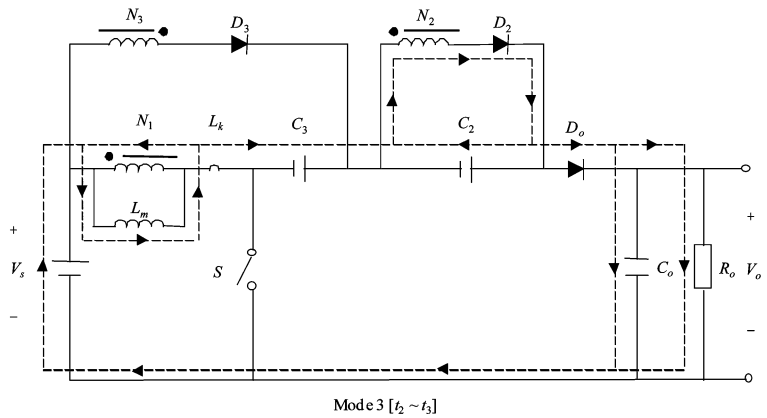

Mode 3 $[t_2 \sim t_3]$

(c)

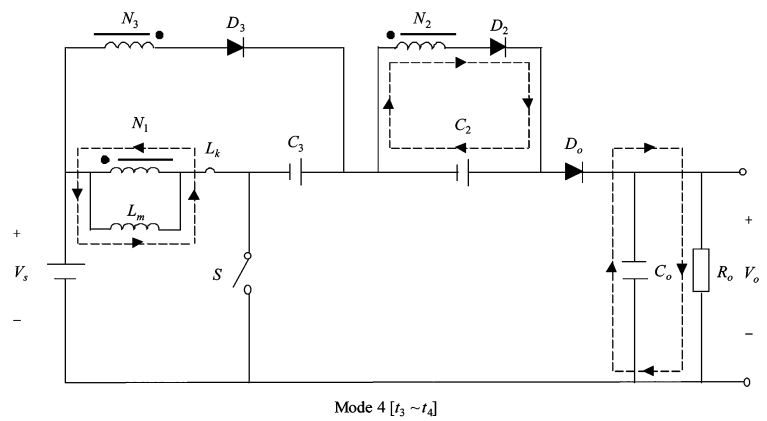

Mode 4 $[t_3 \sim t_4]$

(d)

Fig. 3. Topological modes: (a) mode1 $[t_0 - t_1]$; (b) mode 2 $[t_1 - t_2]$; (c) mode 3 $[t2 - t3]$; (d) mode 4 $[t3 - t4]$.

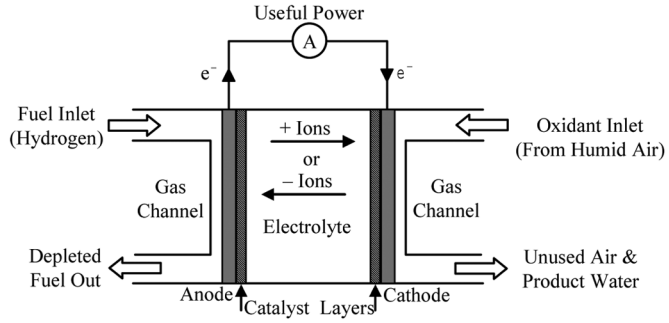

Fig. 4. Fuel cell basic configuration.

Assume that all devices are ideal, the voltages across the clamped capacitors (C_2 and C_3) can be denoted as

$$V_{C2} = -n_2 v_{Lm}(t), \quad t_1 < t < t_4 \tag{17}$$

$$V_{C3} = (1+n_3)V_s. \tag{18}$$

Due to the concept of the zero average voltage across the inductor over one period [4], the voltage gain for steady-state operation can be derived via (6), (9), (17), and (18) as

$$\frac{V_o}{V_s} = (1+n_3) + \frac{1}{1-d} + \frac{d}{1-d}n_2. \tag{19}$$

where d is the duty cycle of the switch (S). Continuously, the switch (S) is turned on at time $t = t_4$ to begin the next switching cycle. According to (19), the voltage gain can be tuned by regulating the turn ratios (n_2 and n_3) in the three-winding coupled inductor to overcome the boost-ratio limitation of the conventional converter. Moreover, the utility rate of magnetic core can be much improved due to the three-winding coupled inductor operated both in the forms of forward and flyback converters.

III. PEMFC Operation Principle

The basic fuel cell concept involves converting chemical energy directly into electrical energy. It produces electricity by electrochemically combining fuel (hydrogen) and oxidant (oxygen from the air) gases through electrodes and across an ion-conducting electrolyte. The fuel cell is composed of two electrodes, an anode, cathode, the catalyst and an electrolyte, as illustrated in Fig. 4 [17]. The main function of the electrode is to bring about a reaction between the reactant and the electrolyte. The anode, used as the negative post in the fuel cell, disperses the hydrogen gas equally over the entire catalyst surface and conducts the electrons for use as power in an external circuit. The cathode, used as the positive post in the fuel cell, distributes the oxygen fed to it onto the catalyst surface and conducts the electrons back from the external circuit. The catalyst is a special material used to facilitate the oxygen and hydrogen reaction. A single cell in constant operating conditions and load can achieve few hundred hour operation but its lifetime usually decreases drastically in real changeable operating conditions. In the choice of fuel, hydrogen may be extracted from natural gas, propane, butane, methanol, and diesel fuel. The energy density of the system (stack+fuel) depends on the type of fuel.

According to the chemical characteristics of the electrolyte used as the ion conductor in the cells, the most promising types are classified as: 1) proton exchange membrane fuel cell (PEMFC) and direct methanol fuel cell (DMFC), which use a polymer membrane as the electrolyte; 2) phosphoric acid fuel cell (PAFC), which uses pure phosphoric acid as the electrolyte; 3) molten carbonate fuel cell (MCFC), which uses a molten mixture, sodium, and potassium carbonates as the electrolyte; 4) SOFC, which uses a ceramic material as the electrolyte [18].

The PEMFC is one of the most promising fuel cell types, and is often considered a potential replacement for the internal combustion engine in transportation applications [18]. The PEMFC consists of porous carbon electrodes bound to a thin sulphonated polymer membrane. The anode, cathode, and net cell reactions of the PEMFC can be represented as

$$\text{Anode Reaction}: \mathrm{H_2} \rightarrow 2\mathrm{H^+} + 2\mathrm{e^-} \tag{20}$$

$$\text{Cathode Reaction}: \frac{1}{2}\mathrm{O_2} + 2\mathrm{H^+} + 2\mathrm{e^-} \rightarrow \mathrm{H_2O} \tag{21}$$

$$\text{Net Cell Reaction}: \mathrm{H_2} + \frac{1}{2}\mathrm{O_2} \rightarrow \mathrm{H_2O} \tag{22}$$

where the mobile ion is $\mathrm{H^+}$. The membrane electrode assembly (MEA) is sandwiched between two collector plates that provide an electrical path from the electrodes to the external circuit. Flow channels cut into the collector plates distribute reactant gases over the surface of the electrodes. Individual cells consisting of collector plates and MEAs are assembled in series to form a fuel cell stack.

Fuel cell generation systems have been receiving more attention in the last years due to the advantages of their high efficiency, low aggression to the environment, no moving parts and superior reliability and durability. Due to the electrochemical reaction, fuel cell has the power quality of low voltage and high current. However, the fuel cell stack with high output voltage is difficult to fabricate and it may be failure when any single cell is inactive. Besides, the output voltage is varied easily with respect to the load variations. In order to satisfy the requirement of high-voltage demand, a stable boost converter with high voltage gain and superior conversion efficiency is necessary in order to utilize the fuel cell energy more efficiently and satisfy the requirement of high-voltage demand in some applications. The validity of the proposed converter in Section II is verified by the following experimental results via an example of a PEMFC power source.

IV. Experimental Results

In order to verify the effectiveness of the designed converter topology, the clean energy of a PEMFC system is utilized for the low-voltage power source in the proposed high-efficiency dc-dc converter and its application circuit is depicted in Fig. 5. In Fig. 5, the fuel cell input is supplemented by an input capacitor C_i (e.g., electrolytic capacitor or ultra-capacitor) that helps for maintaining the bus voltage during transients and startup. The diode D_i at the output of the fuel cell stack is necessary to prevent the negative current going into the stack. Due to the negative current, it is possible that the cell reversal could occur and damage the fuel cell stack. Moreover, the ripple current seen

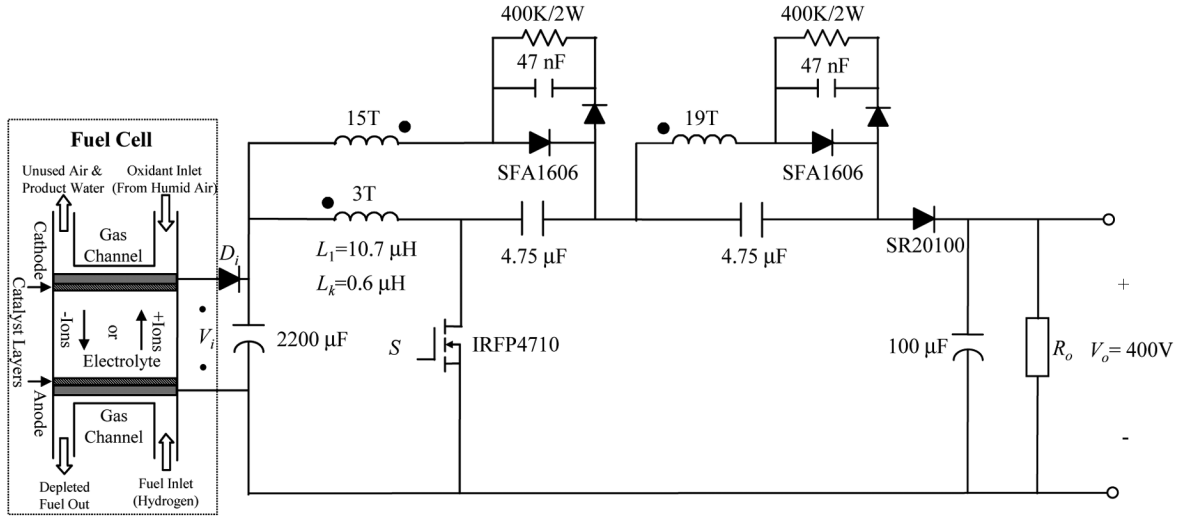

Fig. 5. Application circuit for PEMFC system.

by the fuel cell stack due to the switching of the power conditioning mechanism has an important impact on the durability of the fuel cell. However, it is mainly caused by a dc/ac inverter with drawing an ac ripple current at twice the output frequency. In future inverter integration research, advanced current control methods could be designed to prevent the possible damages caused by the current ripple and the unreasonable cell voltage drops at high current densities. In order to clamp the peak diode voltages caused by the resonance between the leakage inductor of the coupled inductor and the parasitic capacitor of the diodes (D_2 and D_3), two snubber mechanisms are employed. The PEM fuel cell system used in this study is the PowerPEMTM-PS250 manufactured by the Hpower Company. It is a dc power source with 250-W dc nominal power rating. The system operates on ambient air and clean pressurized hydrogen fuel. The fuel cell system consists of a (40) cell stack of the PEM type, mechanical auxiliaries, and electronic control module. In general, the voltage variation of the fuel cell stack is within $\pm 20\%$. According to the converter design and analyses in Section II, the proposed converter circuit is sufficient to deal with this realistic power source with high current density and large voltage variation.

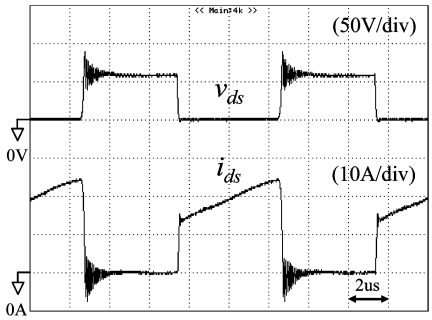

Fig. 6. Experimental voltage and current curves of switch S.

In experimentation, the high-efficiency dc-dc converter is designed to operate from the fuel cell variability dc input, $V_i = 27 - 36.5$ V, to deliver a constant dc output, $V_0 = 400$ V, with the maximum capability of output power, $P_{\text{omax}} = 300$ W. In order to solve the problem of the fuel cell output voltage varied with the variations of loads, the proposed converter with dc voltage feedback control is utilized to ensure the system stability, and a PWM control IC TL494 is adopted to achieve this

---

Switching frequency	$f_s = 100$ kHz;
Turn ratio	$n_2 = 6.33$; $n_3 = 5$;
Inductor	$L_1 = 10.7\ \mu$H; $L_k = 0.6\ \mu$H;
Capacitor	$C_i = 2200\ \mu$F; $C_2 = 4.75\ \mu$F; $C_3 = 4.75\ \mu$F; $C_0 = 100\ \mu$F;
Switch	$S : IRFPS4710(100\text{ V}, R_{\text{DS(on)}} = 14\ \text{m}\Omega)$;
Diode	D_0 : Schottky diode $SR20100(100\text{ V}, 20\text{ A})$;
	$D_2, D_3 : SFA1606(400\text{ V}, 16\text{ A})$.
Weight	1.24 kg
Volume	$2250\ \text{cm}^3(15\text{ cm} \times 15\text{ cm} \times 10\text{ cm})$

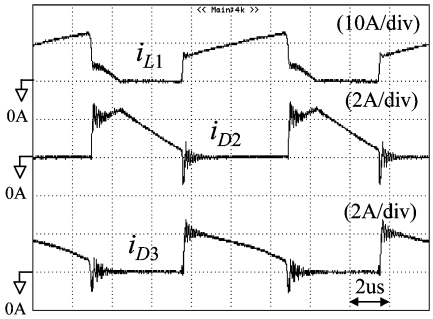

Fig. 7. Experimental current responses of i_{L1}, i_{D2} and i_{D3}.

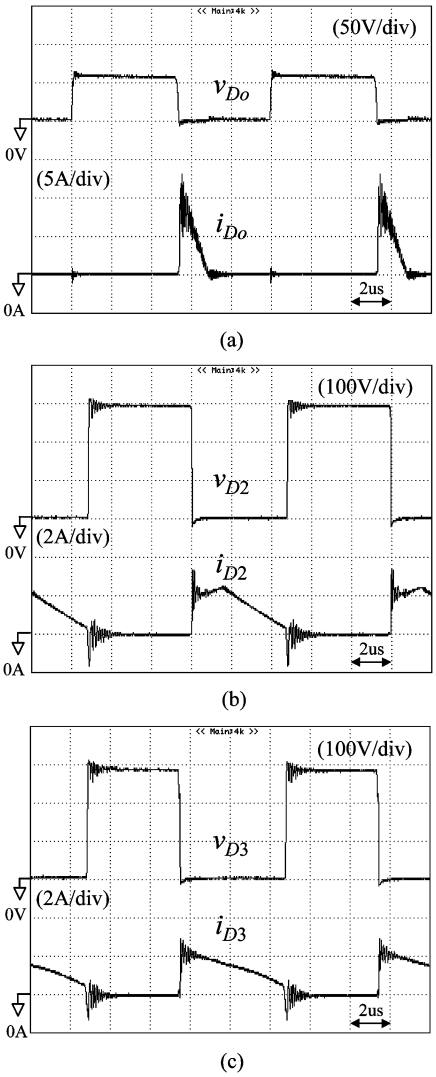

Fig. 8. Experimental voltage and current responses of diodes: (a) D_0; (b) D_2; (c) D_3.

goal of feedback control. The prototype with the following specifications, designed in this section to illustrate the design procedure given in Section II (see equation at the bottom of the previous page). Note that, this application example of a PEMFC with 250-W dc nominal power rating is just used to verify the effectiveness of the proposed converter. In higher power applications, such as the 2003 Future Energy Challenge, the weight and volume of the power conditioner including a dc/dc converter

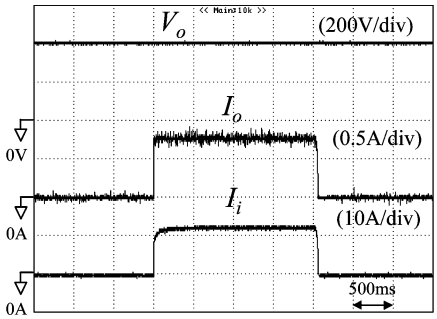

Fig. 9. Experimental results of converter output voltage V_0, output current I_0, and PEMFC output current I_i under step load variation between no-load (0 W) and full-load (300 W).

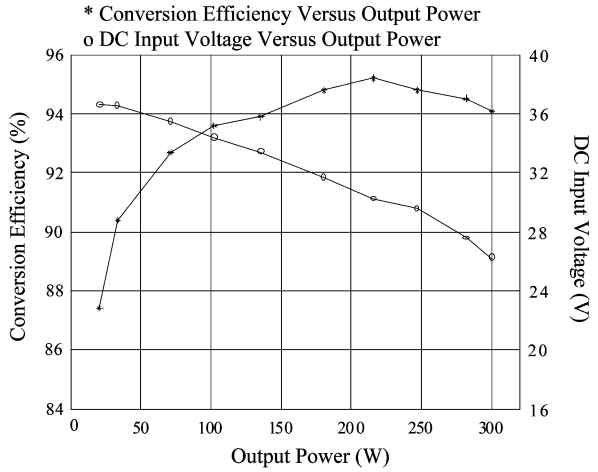

Fig. 10. Converter efficiency and fuel cell voltage under different output powers.

and a dc/ac inverter in a fuel cell generation system should be less than 30kg and 88.5 liters for a 5-kW application. As the proposed topology in this study is extended to higher power demand, the magnetic core should be increased and the copper sheet is necessary to sustain the large current of the primary coil. Of course, the weight and volume will be regularly increased. However, for an isolation-required system, the proposed converter in higher switching frequency could substantially reduce the sizes of the inductor and capacitor compared to thoes in [21].

The measured efficiency of the proposed high-efficiency converter operating at 300-W output power is 94.1%, and the associated experimental results are introduced as follows. Fig. 6 depicts the experimental voltage and current curves of the switch (S). As can be seen from this figure, the shaken switch voltage at the beginning is caused by the line inductor when the switch is turned off. Fortunately, the steady state of this switch voltage stress is about 60 V due to the utilization of voltage-clamped technique and it is much smaller than the output voltage, $V_0 = 400$ V. It has the merit of selecting a low-voltage-rated device in order to reduce the conduction loss of the switch. The experimental coupled-inductor current waveforms of the primary-side (i_{L1}), secondary-side (i_{D2}), and third side (i_{D3}) are depicted in Fig. 7. By observing this figure, the phenomena of the energy transition response in the coupled inductor and the charge current from the third side of the coupled inductor to the capacitor

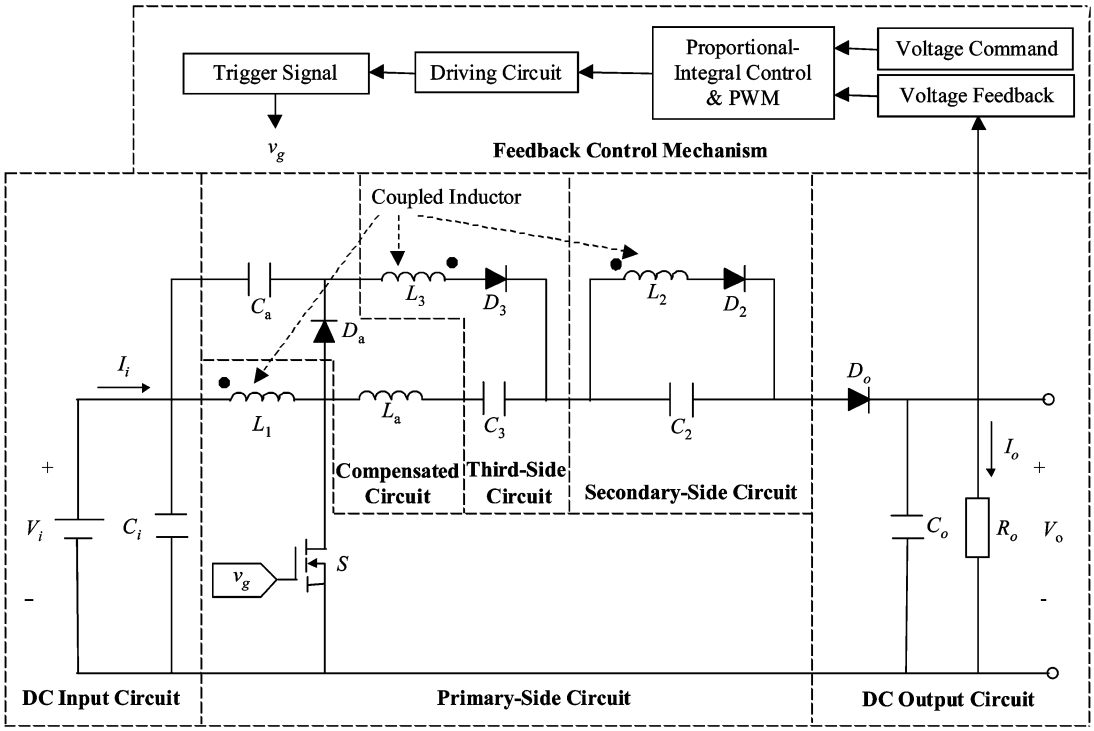

Fig. 11. System configuration of high-efficiency dc-dc converter with compensated circuit.

C_3 are obvious. The experimental voltage and current responses of the diodes (D_0, D_2, and D_3) are depicted in Fig. 8. From these results, the reverse-recovery current in the output diode (D_0) is small to give the credit to the utilization of Schottky diodes with extremely low switching and conduction losses. Thus, it can alleviate the reverse-recovery problem for further raising the conversion efficiency.

In order to examine the robust performance of the proposed converter scheme, the experimental results of the converter output voltage (V_0), output current (I_0), and PEMFC output current (I_i) under the step load variation between no-load (0 W) and full-load (300 W) is depicted Fig. 9. According to Fig. 9, the converter output voltage, $V_0 = 400$ V, is insensitive to the variation of loads due to the closed-loop control, and the output voltage ripple is also slight extremely as a result of high switching frequency. Fig. 10 summarizes the experimental conversion efficiency of the proposed converter and the PEMFC output voltage under different output powers. On the experimental system, the converter efficiency is evaluated via Power Analyzer PA4400A equipment, manufactured by the AVPower Company. The bandwidth of the PA4400A is dc to 500 kHz, and the accuracy of the measured power is within. From the experimental results, the output voltage of the fuel cell decreases as the output power increases due to the load variations and the effects of chemical polarization, concentration polarization, and resistance polarization on cell voltages. In order to solve this phenomenon, the proposed converter with dc voltage feedback control is utilized in this study to ensure the system stability. Moreover, the maximum efficiency is 95.2% at 220–W output power, which is comparatively higher than conventional converters. The above experimental results agree well with those obtained from design procedure given in Section II. However, slight differences in these results are attributed to the factor of system uncertainties in practical applications.

For alleviating the chattering switch voltage in Fig. 6 and the current spike in Fig. 8(a), a high-efficiency dc-dc converter with one compensated circuit is also introduced here and its system configuration is depicted in Fig. 11. The major function of the capacitor, C_a, in the compensated circuit is used for absorbing the leakage energy of the line inductor to lighten the chattering phenomenon of the switch transient voltage. Moreover, it also can further raise the voltage gain of this converter scheme. The aim of the inductor, L_a, in the compensated circuit is utilized for reducing the raising rate of the output-diode current to further diminish the conduction loss. The experimental voltage and current responses of the diodes (D_0 and D_a) via $L_a = 2\ \mu$H, $C_a = 4.75\ \mu$H and D_a with Schottky diode SR20100 are depicted in Fig. 12. Compare with Fig. 8, the current spike of the output diode can be much reduced from 13.5 A to 3.6 A.

V. Conclusion

This study has successfully developed a high-efficiency dc-dc converter with high voltage gain and reduced switch stress, and this converter has been applied well for a PEMFC system with the power quality of low voltage as well as high current. According to the experimental results, the maximum efficiency was measured to be over 95%, which is comparatively higher than conventional converter with the same voltage gain. The newly designed converter circuit has the following improvement compared to the previous works. 1) The voltage gain and the utility rate of magnetic core can be much heightened due to the utilization of a three-winding coupled inductor. 2) It can select the switch with lower sustainable voltage for alleviating the switch

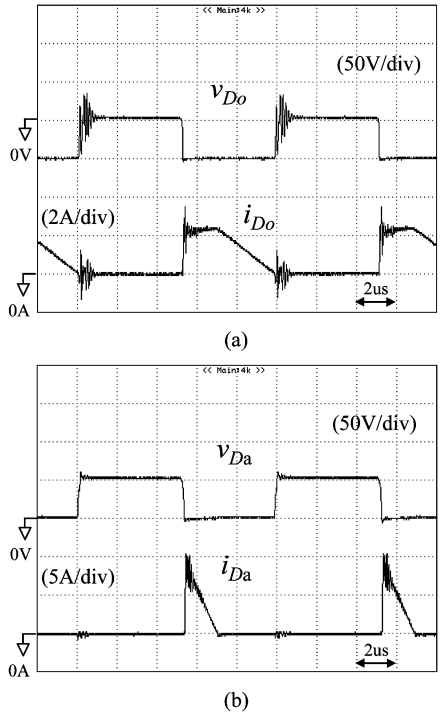

Fig. 12. Experimental voltage and current responses of diodes: (a) D_0; (b)D_a.

conduction loss. 3) The reverse-recovery problem can be solved by the manipulation of the delay time formed with the cross of primary and secondary currents of the coupled inductor. 4) The output diode in this circuit topology can be selected as Schottky diode with the reduction of switching and conduction losses. 5) The voltage drift problem of the power source under the variation of loads can be coped by the closed-loop control methodology. This high-efficiency converter topology provides designers with an alternative choice to convert renewable energy efficiently, and it also can be extended easily to other power conversion systems for satisfying high-voltage demands.

ACKNOWLEDGMENT

The authors would like to express their gratitude to the Referees and the Associate Editor for their useful comments and suggestions.

REFERENCES

[1] I. Barbi and R. Gules, "Isolated DC-DC converters with high-output voltage for TWTA telecommunication satellite applications," *IEEE Trans. Power Electron.*, vol. 18, no. 4, pp. 975–984, Jul. 2003.

[2] O. Abutbul, A. Gherlitz, Y. Berkovich, and A. Ioinovici, "Step-up switching-mode converter with high voltage gain using a switched-capacitor circuit," *IEEE Trans. Circuit Syst. I*, vol. 50, no. 8, pp. 1098–1102, Aug. 2003.

[3] K. C. Tseng and T. J. Liang, "Novel high-efficiency step-up converter," *Inst. Electr. Eng. Proc. Electr. Power Appl.*, vol. 151, no. 2, pp. 182–190, Mar. 2004.

[4] N. Mohan, T. M. Undeland, and W. P. Robbins, *Power Electronics: Converters, Applications, and Design.* . New York: Wiley, 1995.

[5] M. M. Jovanovic and Y. Jang, "A new soft-switched boost converter with isolated active snubber," *IEEE Trans. Ind. Appl.*, vol. 35, no. 2, pp. 496–502, Mar.-Apr. 1999.

[6] C. M. C. Duarte and I. Barbi, "An improved family of ZVS-PWM active-clamping DC-to-DC converters," *IEEE Trans. Power Electron.*, vol. 17, no. 1, pp. 1–7, Jan. 2002.

[7] E. S. da Silva, L. dos Reis Barbosa, J. B. Vieira, L. C. de Freitas, and V. J. Farias, "An improved boost PWM soft-single-switched converter with low voltage and current stresses," *IEEE Trans. Ind. Electron.*, vol. 48, no. 6, pp. 1174–1179, Dec. 2001.

[8] K. Hirachi, M. Yamanaka, K. Kajiyama, and S. Isokane, "Circuit configuration of bidirectional DC/DC converter specific for small scale load leveling system," in *Proc. Inst. Electr. Eng Conf. Power Conversion*, 2002, pp. 603–609.

[9] C. W. Roh, S. H. Han, and M. J. Youn, "Dual coupled inductor fed isolated boost converter for low input voltage applications," *Electron. Lett.*, vol. 35, pp. 1791–1792, 1999.

[10] Q. Zhao and F. C. Lee, "High-efficiency, high step-up DC-DC converters," *IEEE Trans. Power Electron.*, vol. 18, no. 1, pp. 65–73, Jan. 2003.

[11] B. Ivanovic and Z. Stojikovic, "A novel active soft switching snubber designed for boost converter," *IEEE Trans. Power Electron.*, vol. 19, no. 3, pp. 658–665, May. 2004.

[12] R. J. Wai and R. Y. Duan, "High-efficiency DC/DC converter with high voltage gain," *Inst. Electr. Eng. Proc. Electr. Power Appl.*, vol. 152, no. 4, pp. 793–802, 2005.

[13] R. J. Wai, L. W. Liu, and R. Y. Duan, "High-efficiency voltage-clamped DC-DC converter with reduced reverse-recovery current and switch voltage stress," *IEEE Trans. Ind. Electron.*, vol. 53, no. 1, pp. 272–280, Feb. 2006.

[14] R. Kyoungsoo and S. Rahman, "Two-loop controller for maximizing performance of a grid-connected photovoltaic-fuel cell hybrid power plant," *IEEE Trans. Energy Convers.*, vol. 13, no. 3, pp. 276–281, Sep. 1998.

[15] M. D. Lukas, K. Y. Lee, and H. Ghezel-Ayagh, "Development of a stack simulation model for control study on direct reforming molten carbonate fuel cell power plant," *IEEE Trans. Energy Convers.*, vol. 14, no. 4, pp. 1651–1657, Dec. 1999.

[16] ——, "An explicit dynamic model for direct reforming carbonate fuel cell stack," *IEEE Trans. Energy Convers.*, vol. 16, no. 3, pp. 289–295, Sep. 2001.

[17] A. B. Stambouli and E. Traversa, "Fuel cells, an alternative to standard sources of energy," *Renewable Sustainable Energy Rev.*, vol. 6, pp. 297–306, 2002.

[18] M. W. Ellis, M. R. V. Spakovsky, and D. J. Nelson, "Fuel cell systems: Efficient, flexible energy conversion for the 21st century," *Proc. IEEE*, vol. 89, no. 12, pp. 1808–1818, Dec. 2001.

[19] J. M. Correa, F. A. Farret, J. R. Gomes, and M. G. Simoes, "Simulation of fuel-cell stacks using a computer-controlled power rectifier with the purposes of actual high-power injection applications," *IEEE Trans. Ind. Appl.*, vol. 39, no. 4, pp. 1136–1142, Jul. 2003.

[20] K. Green and J. C. Wilson, "Future power sources for mobile communications," *Inst. Electr. Eng. Electron. Commun. Eng. J.*, pp. 43–47, 2001.

[21] *Proc. 2003 Fuel Cell Seminar* Miami, FL, Nov. 2003.

Rong-Jong Wai (M'99–SM'05) was born in Tainan, Taiwan, R.O.C., in 1974. He received the B.S. degree in electrical engineering and the Ph.D. degree in electronic engineering from Chung Yuan Christian University, Chung Li, Taiwan, R.O.C., in 1996 and 1999, respectively.

Since 1999, he has been with the Department of Electrical Engineering, Yuan Ze University, Chung Li, Taiwan, R.O.C., where he is currently a Professor. He is also the Director of the Electric Control and System Engineering Laboratory at Yuan Ze University, and the Energy Conversion and Power Conditioning Laboratory at the Fuel Cell Center. He is a chapter-author of *Intelligent Adaptive Control: Industrial Applications in the Applied Computational Intelligence Set* (CRC, 1998) and the co-author of *Drive and Intelligent Control of Ultrasonic Motor* (Tsang-Hai, 1999), *Electric Control* (Tsang-Hai, 2002) and *Fuel Cell: New Generation Energy* (Tsang-Hai, 2004). He has authored numerous published journal papers in the area of control system applications. His biography was listed in *Who's Who in Science and Engineering* (Marquis, 2004–2007), *Who's Who* (Marquis, 2004–2007), and *Leading Scientists of the World* (International Biographical Centre, 2005), *Who's Who in Asia* (Marquis, 2006–2007), and *Who's Who of Engineering Leaders* (Marquis, 2006–2007). His research interests include power electronics, motor servo drives, mechatronics, energy technology, and control theory applications.

Dr. Wai received the Excellent Research Award in 2000, and the Wu Ta-You Medal and Young Researcher Award in 2003 from the National Science Council, R.O.C. In addition, he was the recipient of the Outstanding Research Award in 2003 from the Yuan Ze University; the Excellent Young Electrical Engineering Award in 2004 from the Chinese Electrical Engineering Society, R.O.C.; the Outstanding Professor Award in 2004 from the Far Eastern Y. Z. Hsu-Science and Technology Memorial Foundation, R.O.C.; the International Professional of the Year Award in 2005 from the International Biographical Centre, U.K., and the Young Automatic Control Engineering Award in 2005 from the Chinese Automatic Control Society, R.O.C.

Chung-You Lin was born in Ping-tung, Taiwan, R.O.C., in 1980. He received the B.S. degree in electrical engineering at Yuan Ze University, Chung Li, Taiwan, R.O.C., in 2004. He is currently working toward the Ph.D. degree in electrical engineering at the same university.

His research interests include resonant theory, power electronics, and renewable energy.

Rou-Yong Duan was born in Nantou, Taiwan, R.O.C., in 1965. He received the B.S. degree from National Kaohsiung University of Applied Sciences, Kaohsiung, Taiwan, R.O.C., in 1986, the M.S. degree from Chung Yuan Christian University, Chung Li, Taiwan, in 1998, and the Ph.D. degree from Yuan Ze University, Chung Li, Taiwan, in 2004, both in electrical engineering. Since 2004, he has been with the Department of Industrial Safety & Health, Hung Kuang University, Tai Chung, Taiwan, where he is currently an Assistant Professor. His research interests include motor servo drives, resonant theory, power electronics, and renewable energy.

Yung-Ruei Chang (M'01) received the M.S. and Ph.D. degrees in electrical engineering from National Taiwan University, Taipei, Taiwan, R.O.C., in 1995 and 2004, respectively.

He is an Assistant Researcher at the Institute of Nuclear Energy Research (INER), Atomic Energy Council, Taiwan, where he has been working since 1996. From 2000 to 2004, he was with the technical transfer project of Taiwan's fourth nuclear power plant development of which he was involved in system reliability and fault-tolerant system design. He spent one year as a Visiting Engineer at STN ATLAS, Germany and GE, USA, in 2000. Since 2005, he has been responsible for power conditioning systems of the renewable energy project at INER. His research interests include system reliability analysis, fault-tolerant system, dependable computing, software reliability, and power electronic system.